CellPress

Immunoglobulin Gene Insertions and Deletions in the Affinity Maturation of HIV-1 Broadly Reactive Neutralizing Antibodies

Thomas B. Kepler,[1,*] Hua-Xin Liao,[2] S. Munir Alam,[2] Rekha Bhaskarabhatla,[1] Ruijun Zhang,[2] Chandri Yandava,[1] Shelley Stewart,[2] Kara Anasti,[2] Garnett Kelsoe,[2,3] Robert Parks,[2] Krissey E. Lloyd,[2] Christina Stolarchuk,[2] Jamie Pritchett,[2] Erika Solomon,[2] Emma Friberg,[2] Lynn Morris,[4,5] Salim S. Abdool Karim,[5] Myron S. Cohen,[6] Emmanuel Walter,[2,7] M. Anthony Moody,[2,7] Xueling Wu,[8] Han R. Altae-Tran,[8] Ivelin S. Georgiev,[8] Peter D. Kwong,[8] Scott D. Boyd,[9] Andrew Z. Fire,[9] John R. Mascola,[8] and Barton F. Haynes[2,3,10]

[1]Department of Microbiology, Boston University School of Medicine, Department of Mathematics & Statistics, Boston University, Boston, MA 02118, USA
[2]Duke University Human Vaccine Institute
[3]Department of Immunology
Durham, NC 27710, USA
[4]Centre for HIV and STIs, National Institute for Communicable Diseases, Johannesburg 2131, South Africa
[5]Center for AIDS Program of Research in South Africa (CAPRISA), Nelson R Mandela School of Medicine, University of KwaZulu-Natal, Congella, 4013, South Africa
[6]University of North Carolina at Chapel Hill, Chapel Hill, NC 27599, USA
[7]Department of Pediatrics, Durham, NC 27710, USA
[8]Vaccine Research Center, NIAID, NIH, Bethesda, MD 20892, USA
[9]Stanford University Medical Center, Stanford, CA 94305, USA
[10]Department of Medicine, Durham, NC 27710, USA
*Correspondence: tbkepler@bu.edu
http://dx.doi.org/10.1016/j.chom.2014.08.006

SUMMARY

Induction of HIV-1 broad neutralizing antibodies (bnAbs) is a goal of HIV-1 vaccine development but has remained challenging partially due to unusual traits of bnAbs, including high somatic hypermutation (SHM) frequencies and in-frame insertions and deletions (indels). Here we examined the propensity and functional requirement for indels within HIV-1 bnAbs. High-throughput sequencing of the immunoglobulin (Ig) V_HDJ_H genes in HIV-1 infected and uninfected individuals revealed that the indel frequency was elevated among HIV-1-infected subjects, with no unique properties attributable to bnAb-producing individuals. This increased indel occurrence depended only on the frequency of SHM point mutations. Indel-encoded regions were generally proximal to antigen binding sites. Additionally, reconstruction of a HIV-1 CD4-binding site bnAb clonal lineage revealed that a large compound V_HDJ_H indel was required for bnAb activity. Thus, vaccine development should focus on designing regimens targeted at sustained activation of bnAb lineages to achieve the required SHM and indel events.

INTRODUCTION

With the use of antigen-specific memory B cell isolation and antibody rescue techniques, a large number of HIV-1 broad neutral-izing antibodies (bnAbs) have been isolated (Haynes et al., 2011). All bnAbs share one or more unusual traits such as autoreactiv-ity, long heavy-chain third complementarity-determining regions (HCDR3s), and high levels of somatic hypermutation (Walker et al., 2009,2011; Haynes et al., 2005, 2012; Kwong and Mas-cola, 2012; Mouquet and Nussenzweig, 2012; Wu et al., 2010, 2011; Zhou et al., 2010; Mascola and Haynes, 2013; Liao et al., 2013), all traits that can limit the induction of such antibodies (Haynes et al., 2005, 2012; Mascola and Haynes, 2013; Verkoczy et al., 2011).

Some recently isolated HIV-1 bnAbs have been noted to possess another unusual characteristic: multibase in-frame in-sertions or deletions (indels) (Wu et al., 2010; Walker et al., 2011). Indels are introduced during somatic hypermutation and are thus found exclusively in germinal center or postgerminal center B cells (Fukita et al., 1998). The proportion of indels among somatic mutations in the normal human B cell repertoire is small. Wilson et al. examined IgG memory cells from human tonsil and reported six indels in 110,000 bases sequenced from productive genes, comprising both 3- and 6-base insertions and deletions (Wilson et al., 1998). Using high-throughput sequencing, Briney et al. (2012) found slightly higher frequencies of in-frame inser-tions (1.8% of all sequences) and in-frame deletions (2.0%–2.6% of all sequences) in FACS-sorted memory B cells. Smith et al. (1996) studied unselected mutations in the introns between the JH and constant region genes and found that 1%–2% of all unselected somatic mutations were single-base insertions or de-letions. When indels do occur in normal B cells, they are usually short; their frequency decreases rapidly with length (Wilson et al., 1998). Here we have surveyed bnAb sequences and found that 40% of reported HIV-1 bnAbs have indels and that the indel sizes cover the remarkable range from 3 to 33 nucleotides.

CrossMark

Table 1. Insertions and Deletions in Broadly Neutralizing Anti-HIV-1 Antibodies

Antibody	Indel Type	Length	Location
CAP206-CH12	Deletion	3 aa	HFR3
NIH45-46	Deletion	6 aa	LCDR1
HJ16	Deletion	3 aa	HCDR2
HJ16	Insertion	3 aa	LFR3
VRC01	Deletion	6 aa	LCDR1
VRC03	Insertion	21 aa	HFR3
CH98	Deletion	15 aa	LFR1
CL103	Deletion	9 aa	LFR1
PGT121-3	Insertion	9 aa	LFR3
PGT125-8	Insertion	18 aa	HCDR2
PGT125-8	Deletion	15 aa	LCDR1
PGT136	Insertion	3 aa	HCDR2
PGT135-7	Insertion	15 aa	HCDR1
PGT135-7	Insertion	3 aa	LFR1
PGT145	Deletion	3 aa	HCDR3
PG9	Insertion	3 aa	HFR1
CH30-34	Insertion	27 aa	HCDR1
3BNC117, 3BNC60	Insertion	12 aa	HFR3
3BNC117, 3BNC60	Deletion	12 aa	LCDR1
8ANC131, 8ANC134	Deletion	3 aa	HCDR2
8ANC131, 8ANC135	Deletion	3 aa	LCDR1
8ANC195	Deletion	3 aa	HCDR1
8ANC195	Insertion	15 aa	HCDR2
8ANC195	Insertion	3 aa	LCDR1
VRCPG04,04B	Deletion	9 aa	LCRD1
VRCPG04,04B	Insertion	3 aa	HCDR1
VRCPG04,04B	Insertion	3 aa	HFR3

Because induction of bnAbs may be central to HIV-1 vaccine development efforts, it is of great interest to determine why indels occur at such great frequency in bnAbs. There are several hypotheses regarding the cause of this striking bias. Perhaps patients who produce bnAbs have an underlying propensity to incorporate indels during affinity maturation. Another possibility is that chronic HIV-1 infection induces the generation of indels and that indels will be found at greater frequencies in all HIV-1-infected patients. It is also possible that there are genetic polymorphisms that affect the somatic hypermutation mechanism and predispose carriers to produce high levels of somatic hypermutations and indels during the induction of bnAbs. If genetic polymorphins are the cause for elevated SHMs, it would have serious consequences for the development of vaccines to elicit bnAbs, in that only those with such a genetic background will be able to make vaccine-induced bnAbs. In addition, it is important to know whether indels can be required for bnAb activity. To test these ideas, we examined heavy-chain sequences from HIV-1-infected individuals who make bnAbs, as well as from HIV-1-infected individuals who do not. To determine the functional consequences of insertion/deletion events, we made a detailed reconstruction of a VRC01-like CD4 binding site bnAb (CH31) clonal lineage and demonstrated that a large compound indel

was essential for both bnAb affinity maturation and HIV-1 neutralization.

Indels Are Found at High Frequency among HIV-1 bnAbs

Many of the recently isolated bnAbs have been observed to have insertions or deletions. To determine whether the occurrence of indels in bnAbs is disproportionally high, we examined the reported 56 HIV-1 bnAb gene pairs (Table S1), which constituted 26 sets of clonally related heavy- and light-chain genes. Among these genes, we identified 27 unique in-frame indels. Half of these indels were 3 nt long, but insertions as large as 33 nt and deletions up to 15 nt were also observed (Table 1). Overall, 40 of the 108 bnAb genes contained indels. Counting unique indels only, the frequency of indels in this group of genes was 27/108 (25%). This rate is nearly seven times higher than that observed in a collection of ~13,000 human heavy-chain variable regions downloaded from NCBI GenBank. Thus, the frequency of indels among bnAbs is elevated.

To determine whether the high frequency of indels in bnAbs was attributable to an increase in the frequency of indel-bearing antibodies generally in all chronically infected HIV-1-infected individuals, versus selective increase of indels in bnAb-producing individuals, we determined the frequency of indels in unbiased samples of Ig variable region genes from blood B cells using Roche 454 high-throughput DNA sequencing (HTS) of full-length genomic V_HDJ_H rearrangements. We generated and analyzed HTS data comprising 3,778,439 sequencing reads from 261 samples taken at different times from 75 human subjects. These individuals included 41 HIV-infected individuals (8 bnAb producers and 33 non-bnAb producers), 18 influenza-vaccinated individuals, and 16 HIV-1-uninfected individuals (Tables S2 and S3).

After discarding sequences rearranged out of frame or containing frame-shifting indels, we analyzed a total of 3,352,720 sequences using statistical methods and software developed for this purpose (Kepler, 2013). All alignments between sequencing reads and gene segments used an affine gap scoring function (Gotoh, 1990). Each sequence was scored either as containing or not containing an in-frame insertion and/or deletion.

We found that V_HDJ_H genes from HIV-1-infected bnAb and non-bnAb subjects have higher levels of indels than do those from healthy influenza-vaccinated and non-HIV-1-infected groups (Figures 1A and 1B). Compared to non-HIV-1-infected subjects, the geometric mean insertion frequency was 27% higher in HIV-1-infected individuals (p = 0.03; ANOVA); the geometric mean deletion frequency was similarly 23% higher in HIV-1-infected individuals (p = 0.03; ANOVA). Importantly, with HIV-1-infected individuals, indel frequencies did not significantly differ between bnAb-producing and nonproducing subjects (p > 0.1 in both cases; Tukey multiple-comparisons test).

Mean Indel Frequency Is Predicted by Mean Mutation Frequency

The frequency of point mutations is similarly elevated in HIV-1-infected individuals (ANOVA p < 0.01 for differences attributable to subject classification; Tukey multiple comparisons, p < 0.05 for differences specific to HIV-1 status). This result raises the possibility that both point mutation and indel frequencies are increased together by the same underlying cause. We hypothesized that since indels are induced by the same mechanism as
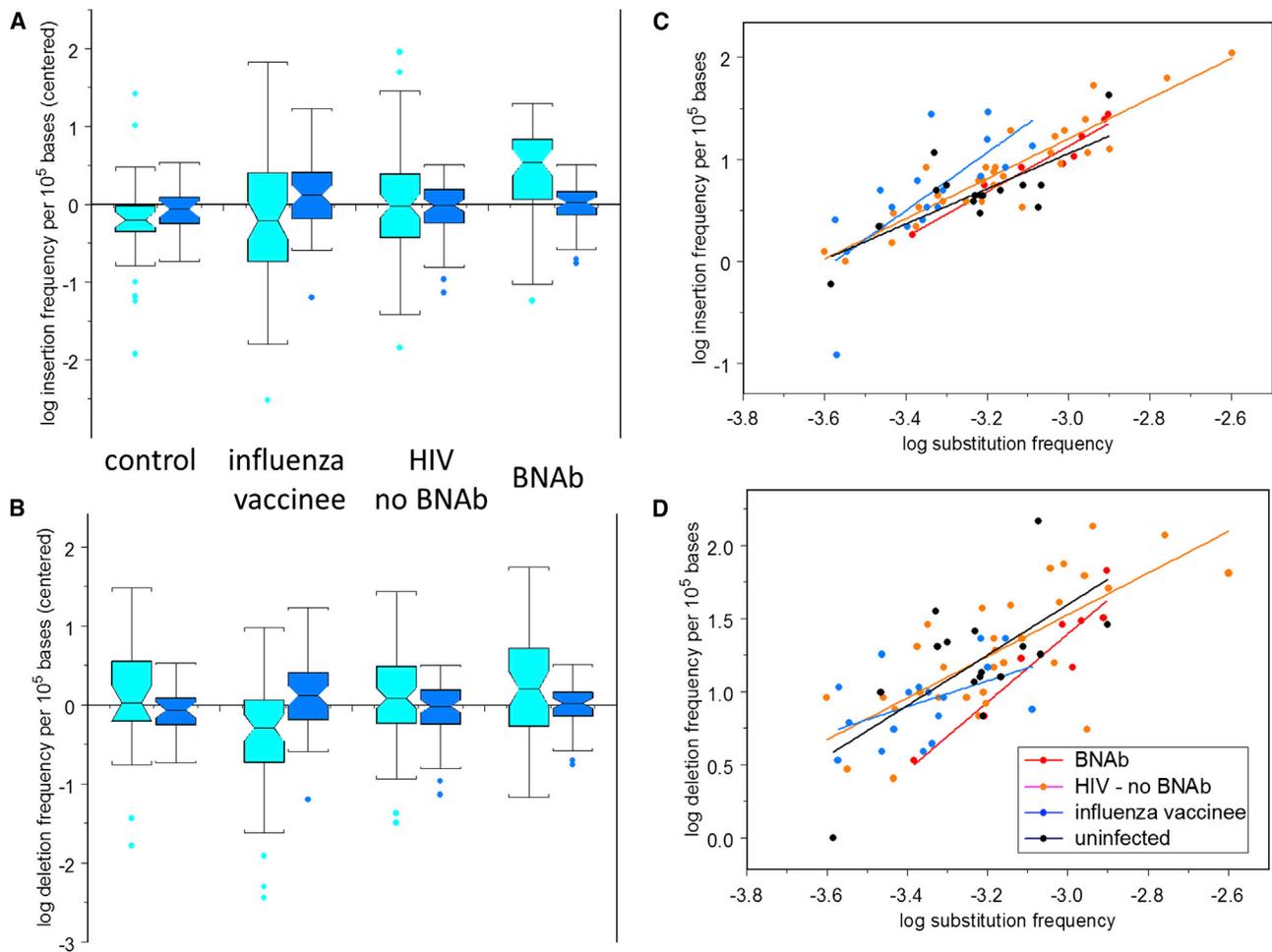
Figure 1. Comparison of VH Mutation Frequencies in HIV-1 bnAbs with Those in Other Antibodies

(A and B) Box plots showing centered log frequencies (cyan) for in-frame insertions (A) and deletions (B) per 10^5 VH bases in potentially functional heavy-chain genes, and insertion and deletion log frequency residuals (blue) after subtracting log frequency predicted from substitution frequency alone. Subject classifications: subjects known to produce broadly neutralizing antibodies against HIV-1 (bnAb), subjects who had been vaccinated against influenza 1 week prior to sampling (influenza vaccinee), HIV-1-infected subjects who had not produced bnAbs by the time of this study (HIV no bnAb), and uninfected controls (control). Boxes cover from the first to the third quartiles; whiskers extend to the standard span—1.5 times the interquartile range. Cyan boxes were centered by subtracting the mean frequency over all subjects; blue boxes were not centered.

(C and D) Log of the insertion frequency per 10^5 bases (C) and deletion frequency (D) as a function of the log of the substitution frequency per base. The colored line segments show the linear regression for each of the subject classifications; the gray line segment shows the linear regression for all subjects at once.

point substitutions, a higher overall mutation level could account for the higher indel frequency. To evaluate this possibility, we performed linear regressions of log average insertion or deletion frequency against the log of the substitution frequency. The regressions were performed with separate regression coefficients for each subject classification group as well as with a common regression coefficient for all subjects. The regression coefficients were not statistically different among subjects for either insertions or deletions ($p > 0.1$, ANOVA; Figures 1C and 1D); the estimate ($\pm$SE) for the common regression coefficient was 1.95 ± 0.13 for insertions and 1.44 ± 0.22 for deletions. Figures 1A and 1B also show the residuals remaining after subtracting the insertion and deletion frequencies predicted using the common-coefficient regression models, illustrating that most of the variability among classifications was attributable to differences in point substitution frequency.

We were able to study nine HIV-1-infected individuals (five among the bnAb-producers and four among the non-bnAb producers) with $V_H D J_H$ sequencing data from three or more sampling times. The frequency of indel-containing sequences was variable over time (Figure 2). Simple linear regression of insertion or deletion frequencies against days postinfection found regression coefficients for insertion significantly greater than zero in two out of nine cases ($p < 0.05$), while eight out of nine regression coefficient estimates were positive, significantly more than expected if there were no temporal trend ($p = 0.004$, two-sided sign test). No such trend was evident for deletions—no correlation coefficients differed statistically from zero, and four out of nine were positive. Although indel frequency is volatile, there is a weak but detectable tendency for insertions, but not deletions, to increase over time with HIV infection.
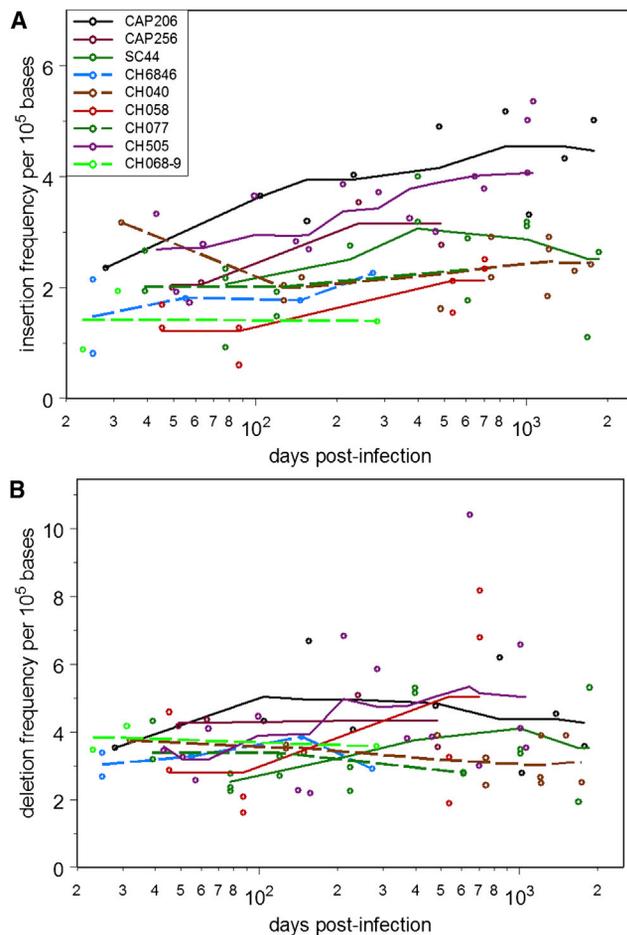
Figure 2. Time Course of In-Frame Insertion and Deletion Frequencies in Days Postinfection for HIV-Infected Subjects

Time course of in-frame insertion (A) and deletion (B) frequencies. The five subjects known to produce bnAbs are indicated with solid lines; the four who have not made bnAbs are indicated with dashed lines. Only subjects with samples taken at three or more times were included.

To address the question of whether chronic infections other than HIV are associated with increased rates of insertions and deletions, we examined HTS heavy-chain Ig repertoire data from subjects chronically infected with cytomegalovirus (CMV), Epstein-Barr virus (EBV), both viruses, or neither (Wang et al., 2014). There were no detectable differences among these groups in the rates of in-frame insertions or deletions (p > 0.1, ANOVA; Figure S2).

Indel Placement and Antigen Recognition

To determine whether indels in bnAbs were preferentially found in antigen-interacting regions or were more randomly distributed, we analyzed a set of 11 antigen-bound bnAb structures containing a total of 18 indels (Supplemental Experimental Procedures). Fifteen of 18 (83%) indels were found within 10 Å of the respective antigen binding site (Figure 3). In comparison, analysis of loop regions (assumed to be able to more easily accommodate indels due to fewer structural constraints compared to beta strand regions) revealed that only approximately one-third of loop residues were found within 10 Å of the respective antigen, even when removing potential skewness due to overrepresentation of specific antibody classes (Figure S1). The distributions of the indel and loop residue locations were significantly different (p < 0.0001, Mann-Whitney test). These results indicated that while there was little constraint on the location where indels can be accommodated, their presence related directly to antigen recognition. One potential caveat of this analysis is that proximity to antigen was measured based on the Env subunit antigen constructs in the available crystal structures, rather than a functional HIV-1 spike, thus possibly underestimating the proximity to antigen for some indels. Overall, indels were preferentially found in close proximity to antigen binding sites, and thus likely improved interactions with antigen.

The Indel in VRC01-like CD4 Binding Site CH30-CH34 Clonal Lineage Was Required for bnAb Affinity Maturation

We have recently reported the occurrence of two different sets of clonally related bnAbs in the same HIV-1-infected individual that together accounted for all of the plasma bnAb activity (Wu et al., 2011; Bonsignori et al., 2012). This individual (CH0129) had both VRC01-like CD4 binding site and V1V2 quaternary bnAb activity (Bonsignori et al., 2011, 2012). The VRC01-like CD4 binding-site clone CH30–CH34 experienced indel formation, while the V1V2 PG9-like bnAb clonal lineage CH01–CH04 did not. We reconstructed the corresponding CH31 clonal lineage using statistical inference on the originally isolated genes, supplemented with targeted HTS reads to determine the affinity maturation history and the role of indel in affinity maturation and acquisition of neutralization breadth in the observed CH31 lineage CD4bs antibodies (Figure 4; Table 2).

The members of the CH31 clonal lineage are similar to other VRC01-like bnAbs clone in their use of the VH1-2*02 gene segment (Wu et al., 2011; Bonsignori et al., 2012). Moreover, the crystal structure of CH31 complexed to gp120 is superimposable on that of VRC01 (Zhou et al., 2013). Most strikingly, perhaps, is the observation that both VRC03 (a member of the VRC01 clonal lineage) and all the members of the CH31 clonal lineage contain large indels. VRC03 has a 21 nt insertion in framework region 3. The CH31 clonal lineage genes have a net 27 nt insertion within CDR1 that resolves into a 6 nt deletion and a 33 nt tandem duplication (Figure 4A). Using HTS targeted at $V_H D J_H$ genes rearranging to the V_H and J_H gene segments used by CH31 lineage antibodies, we were able to isolate genes situated close to the inferred unmutated common ancestor (UCA) on the clonal tree and prior to the indels. Importantly, we isolated 14 unique $V_H D J_H$ genes that were clearly members of the CH31 clonal lineage but did not have the indel, as well as isolated several hundred more mutated $V_H D J_H$ genes that did have the indel (Figure 4C).

The CH31 clonal lineage history demonstrated a striking accumulation of mutations in the vicinity of the eventual indel, including the formation of an activation-induced cytidine deaminase (AID) AGC hotspot that probably contributed to the genetic instability responsible for the indel (Figure 4A). Indeed, a feature common to all of the bnAbs that have experienced indels is an accumulation of point mutations on either side of the insertion or deletion (Figure S1).
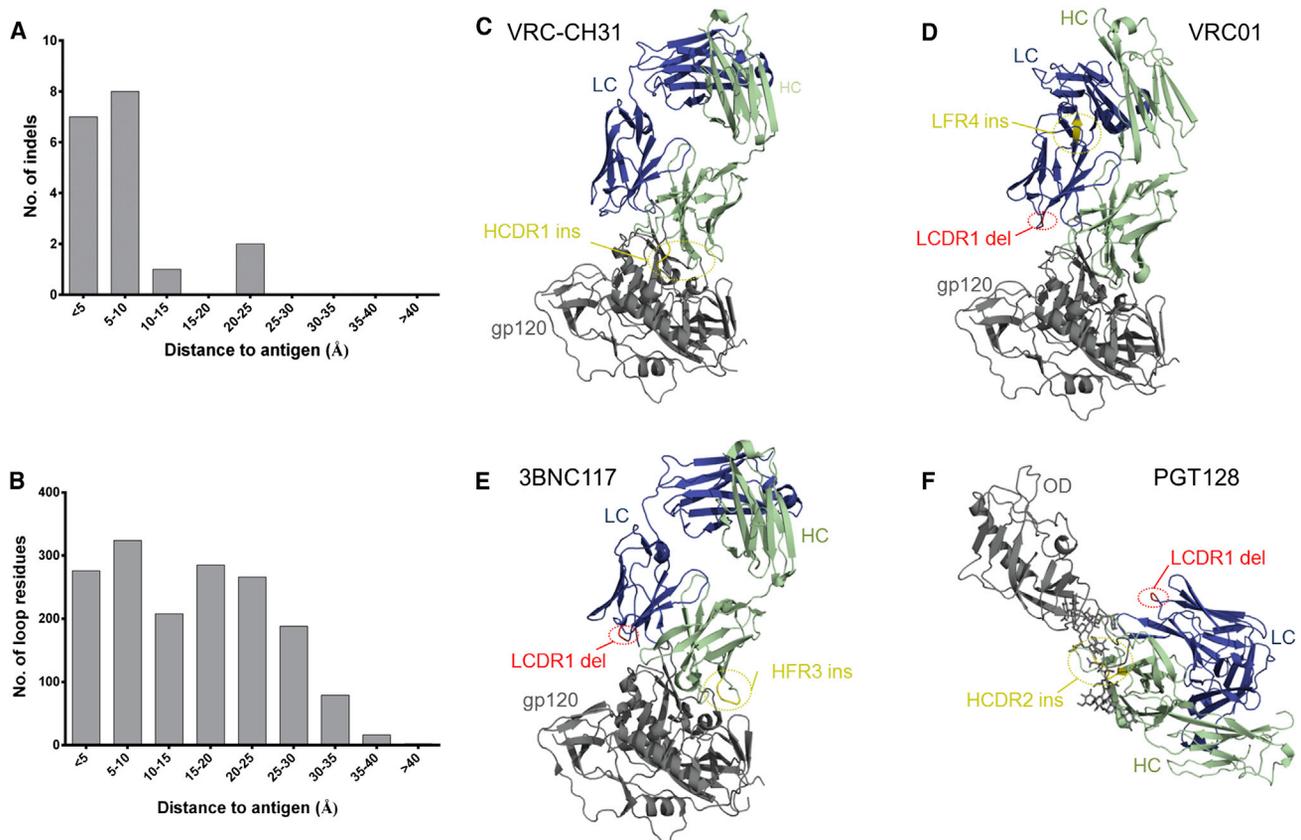
Figure 3. Structural Analysis of Antibody Indels

(A and B) Distribution of distances between antigen and indels (A) or loop residues (B). These distributions are statistically distinguishable (p < 0.0001, Mann-Whitney test). Distances are shown as bins in 5 Å increments.

(C–F) Location of insertions and deletions in antigen-bound structures of antibodies VRC-CH31 (C), VRC01 (D), 3BNC117 (E), and PGT128 (F). Structures are shown in ribbon representation with antibody heavy chains in green, light chains in blue, and the respective antigens in gray. For PGT128, antibody-interacting glycans on antigen are shown as gray sticks. The regions where insertions and deletions were observed are highlighted in yellow and red, respectively. See also Figure S1.

We next expressed antibody members of the CH31 clonal lineage representative of key stages along the maturation pathway as well as four artificial heavy-chain constructs (Figure 4B) that were intended to probe the specific contributions of the indel to the affinity, kinetic parameters, and neutralization capacity of CH31 bnAb lineage antibodies generated before and after indel occurrence.

Consider the line of descent leading from the UCA to the mature antibodies CH30–CH34 (Figure 4B). GNM7S is an observed heavy-chain sequence lying just off the line of descent. It arose just before the indel was acquired and is the indel-free sequence farthest from the UCA. Among postindel sequences, H162G is closest to the UCA along the line of descent. GNM7S and H162G differ by 16 nucleotide substitutions in addition to the indel. The differences between the two in terms of their biophysical properties are likely due both to the indel and the nucleotide substitutions. To isolate the influence of the indel from the influence of the simple substitutions, we designed and synthesized four heavy chains that represent hybrids of antibodies H162G and GNM7S involving inclusion or removal of the tandem duplication.

The relationships between the observed and synthetic sequences are shown schematically in Figure 4B. Each heavy chain sequence can be decomposed into three elements: the duplicated element, or *duplicon* (Eichler, 1998), and the elements 5′ and 3′, respectively, of the duplicon. The 5′ element is denoted A, the duplicon D, and the 3′ element B. The structure of GNM7S is given by $A_0 D_0 B$ and that of H162G is $A_1 D_1 D_2 B$. The duplicons D_0, D_1, and D_2 are homologous 33 nucleotide tracts that differ from each other by 5–13 nucleotides. A_0 and A_1 differ from each other by 17 nucleotide substitutions and a 6 nucleotide deletion. GNM7S and H162G share an identical B element. The following four antibody heavy chains were synthesized by adding a duplicon to GNM7S ($A_1 D_1 D_0 B$ and $A_1 D_0 D_2 B$) or deleting a duplicon from H162G ($A_1 D_1 B$ and $A_1 D_2 B$). Each artificial heavy chain was paired with the light chain of a statistically inferred postinsertion antibody for full antibody expression.

We estimated antibody binding kinetic parameters affected by the indel by surface plasmon resonance (SPR) analysis of CH31 lineage members binding to HIV-1 AE.A244 gp120 (Alam et al., 2013). Figure 5 shows that, in the natural CH31 lineage, the association rate of lineage antibodies for AE.A244 gp120 binding
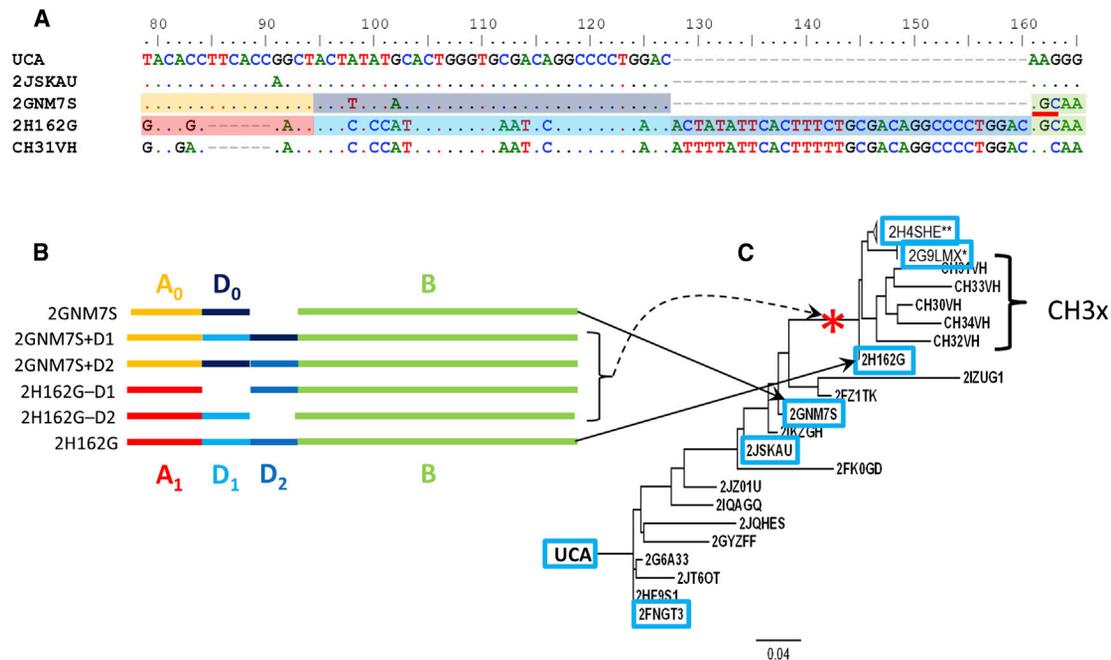
Figure 4. Maturation Pathway of CD4BS bnAb CH31 Clonal Lineage

(A) Alignment of the observed CD4BS bnAb CH31 and observed CH31 clonally related $V_H D J_H$ sequences from HTS shows the likely duplication and deletion events leading to the mature antibody. An AID hot spot "AGC" at alignment position 162 (red line segment) appears as a result of nucleotide substitution in 2GNM7S. Dots indicate identity with the nucleotides in the UCA; dashes represent gaps. Shading of the sequences corresponds to the schematic deconstruction in (B).

(B) A schematic showing the structures of the observed heavy chains (2GNM7S, 2H162G) in terms of the sequence elements A, A'; D_0, D_1, D_2, and B, and the artificial constructs made by inserting and deleting the duplicons.

(C) A maximum-likelihood tree incorporating all antibody members (CH30–CH34) of the CH31 clonal lineage $V_H D J_H$ and the $V_H D J_H$ isolated by HTS. The $V_H D J_H$ genes indicated in blue boxes have been synthesized and paired with intermediate-4 light chain for production of recombinant monoclonal antibodies for testing the binding and neutralizing activity. The compound insertion-deletion event occurred on the branch indicated by the red asterisk. The asterisks on the sequence titles 2H4SHE and 2G9LMX indicate that each of these sequences has hundreds (**) or tens (*) of closely related sequences not shown on the tree.

increased and the dissociation rate decreased with evolutionary distance (in expected number of mutations per base) from the inferred UCA. The artificial antibody constructs in which an indel duplicon was inserted but no other changes made showed that this single change brought about an 8-fold increase in the association rate (Figure 5A). When the indel duplicon was deleted from the postindel heavy chain, the association rate of the antibody for binding to AE.A244 gp120 decreased by an order of magnitude (2H162G-D1; Figure 5A). The dissociation rate was slightly decreased by insertion of the duplicon from 2GNM7S to both 2GNM7S+D1 and 2GNM7S+D2. Upon its deletion, however, the dissociation rate was increased 3-fold (2H162G-D1; Figure 5B). No antibodies less diverged than 2JSKAU from the UCA showed binding of any measurable degree to AE.A244 gp120 (data not shown).

Broad Neutralization by CH31 Antibody Is Acquired after Indel Formation

Finally, we assayed members of the CH31 clonal lineage for their ability to neutralize heterologous HIV-1 strains in the TZBbl neutralization assay (Table 2). We found that neutralization breadth did not arise until after the occurrence of the indel. The only tier 2 (difficult to neutralize) strain neutralized before the indel was A.Q23, with neutralization of other strains only acquired

after the indel with antibodies 2H162G and 2H4HE representing the point in the CH31 lineage with neutralization breadth.

DISCUSSION

In this study, we have demonstrated the high frequency of indels among HIV-1 broad neutralizing antibodies, showed that these indels occur predominantly near bnAb antigen contact sites, and demonstrated an example of the requirement for an indel for affinity maturation and bnAb activity in the VRC01-like CH31 bnAb lineage.

Not all HIV-1-infected individuals make bnAbs, although it has recently been shown that the ability to make BnAbs is not dichotomous. That is, serum neutralization breadth is graded among infected individuals (Hraber et al., 2014). What is not yet known is whether there are host factors such as a genetic predisposition that are responsible for the differences there are. Alternatively, there may be as-yet-undetermined differences in the circumstances of the infection itself, such as total antigenic variability or viral load that drives bnAb production. On the other hand, there may be no host or pathogen factors that determine bnAb status. Instead, bnAb status may be stochastic, driven essentially by the stochastic nature of B cell affinity maturation itself. In this study, we demonstrate that insertion and deletions occur

Table 2. Neutralization of HIV-1 Tier 1 and 2 Isolates by Members of CD4BS bnAb CH31 Clonal Lineage

Antibody	B.MN.3	C.MW965	B.SF162	B.W61D	C.C3347	C.DU172	A.Q23	A.TRO.11	MuLV
	TCID50, ug/ml								
	HIV-1 Isolates								Control
UCA	>50	>50	>50	>50	>50	>50	>50	>50	>50
2FNGT3	>50	>50	>50	>50	>50	>50	>50	>50	>50
2JSKAU	>50	>50	>50	>50	>50	>50	1.51	>50	>50
2GNM7S	30.1	>50	>50	>50	>50	>50	6.57	>50	>50
2H162G	0.03	6.78	1.07	2.62	10.4	5.61	0.08	0.94	>50
2H4SHE	<0.023	2.45	0.402	0.023	3.86	1.63	0.085	0.75	>50
2G9LMX	<0.023	1.43	0.443	0.326	6.48	7.7	0.07	0.95	>50
I1	3.86	10.2	1.34	>50	0.98	0.91	<0.23	0.46	>50
I2	7.19	15.8	1.68	>50	0.77	1.03	<0.23	0.54	>50
I3	5.55	9.09	1.12	>50	0.46	0.71	<0.23	0.47	>50
I4	2.26	5.38	0.77	>50	0.34	0.61	<0.23	0.33	>50
CH31	0.0225	0.993	0.121	8.34	0.17	1.15	<023	0.15	>50
2H162G – D1	>50	>50	>50	>50	>50	>50	3.19	>50	>50
2GNM7S+D.1	14.3	>50	49.7	38.3	>50	>50	4.21	>50	>50
2GNM7S+D2	16.2	>50	27.4	5.8	>50	>50	25.0	>50	>50

at unusually high frequencies among bnAbs and that the occurrence of indels in HIV-1 bnAbs is determined by the degree of SHM that occurs in HIV-1 infection, rather than by the action of factors specific to those patients that have detectable plasma bnAbs. By examining a total of 3,352,720 genomic DNA sequencing reads from individuals with and without HIV-1 infection, we found that the rate of indels could be accounted for by a single mutation frequency driving both point substitution and indels in all groups, with only this single mutation frequency varying among groups. Furthermore, the frequencies of both indels and substitutions were only slightly higher in HIV-1-infected patients, and there was no statistically significant difference between HIV-1-infected patients who have detectable plasma bnAbs and those who did not. Moreover, we found that the indel frequency depends on the substitution frequency raised to a power greater than one. Mathematically, the relationship between the frequency of insertions or deletions f and the frequency of substitutions μ is given by

$$f = \gamma \mu^{\beta}$$

where $\beta > 1$. The interpretation of this finding is that the excess SHM frequency of bnAbs is sufficient by itself to account for the increase in indel frequency. Thus, high indel frequency does not represent a separate class of bnAb anomaly and does not implicate unknown host factors or genetic predisposition to generate bnAbs. In this regard, we have recently performed full exon sequencing on 50 bnAbs and 50 non-bnAbs HIV-1-infected individuals and demonstrated no genome-wide gene maturation associated with the ability to make bnAbs (P. Shea, B.F.H., and D.B. Goldstein, unpublished data).

Previously, Krause et al. (2011) investigated the role of an insertion in a human antibody against influenza HA by deleting the insert while leaving all other somatic mutations intact and comparing binding affinities between the two forms of the antibody. They found that the removal of the insertion increased

the equilibrium dissociation constant 35-fold, largely through increasing the kinetic dissociation rate. Pejchal et al. (2011) deleted the inserts from two gp-120-binding anti-HIV-1 antibodies, while leaving the rest of the molecules intact. They found that the binding affinity for the antigen, and their ability to neutralize the virus, were diminished by the removal of the insert. Our goal and our findings were different from these studies in an important way. While the previous groups of investigators sought to determine the role of the insert in the function of the extant antibodies, we sought to elucidate the role of the insertion event in the affinity maturation of the bnAb clonal lineage. Thus, we isolated lineage members from before and after the compound insertion/deletion event and produced four constructs that represent possible intermediate forms. We found that after an insertion or deletion event, point mutations continue to accumulate in the context of the indel. These postindel mutations may have very different effects in the presence of the indel than they would in its absence. Removing the insert from the mature antibody did not return the antibody to its preindel state because the postindel point mutations were still intact. Our studies more closely approximate the history of the lineage at the time of the indel's occurrence.

Our analyses demonstrate that insertions and deletions are prevalent at very high frequency in bnAbs, that indels can be critical for bnAb activity, and that indel frequency increases with, and is predicted by, the frequency of SHM-mediated substitution. The last point is important because it suggests that the continued accumulation of point mutations in HIV-infected individuals naturally leads to more substantial sequence alterations, such as insertions and deletions, without additional genetic predispositions. It follows that a vaccine strategy specifically designed to target and persistently activate bnAb precursors and their descendants (Haynes et al., 2012) can induce the full spectrum of antibody somatic hypermutations seen in bnAbs and may induce bnAbs as well.
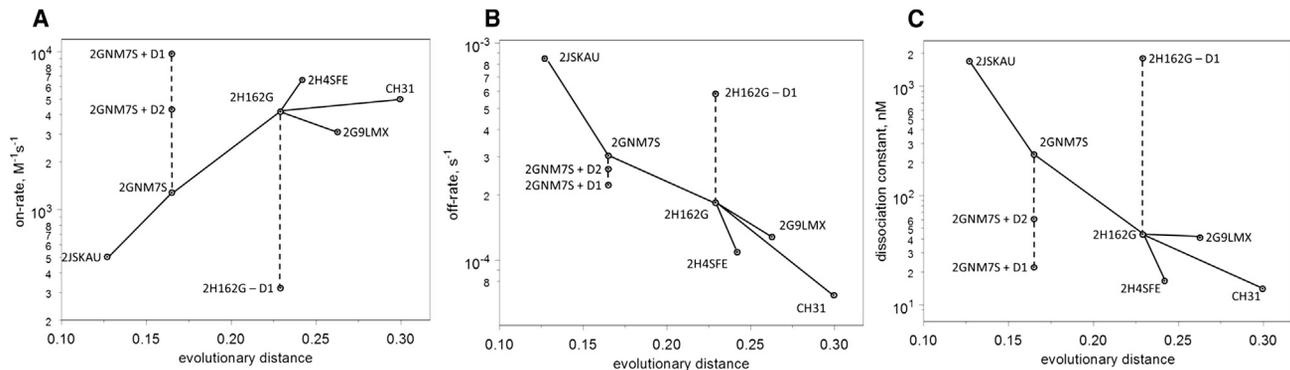
Figure 5. SPR-Estimated Kinetic Rate Constants

(A) Association rate, k_a.

(B) Dissociation rate, k_d for the tested antibodies as a function of evolutionary distance (expected nucleotide changes per base) from the inferred unmutated common ancestor (UCA). Solid line segments indicate clonal descent. Dashed line segments indicate artificial descent by insertion or deletion of the respective duplicon.

(C) The estimated dissociation, K_d (the ratio of the on rate to the off rate, $K_d = k_d/k_a$) versus the evolutionary distance from the UCA.

EXPERIMENTAL PROCEDURES

Human Samples

DNA samples prepared from a total of 261 peripheral blood mononuclear cell (PBMC) samples from 75 human subjects for analysis of $V_H DJ_H$ by HTS. These individuals included 41 HIV-infected individuals (8 bnAb producers and 33 non-bnAb producers) (Shen et al., 2009; Tomaras et al., 2011; Morris et al., 2011; Moore et al., 2011), 16 healthy uninfected individuals, and 18 healthy individuals vaccinated with the 2007–2008 or 2008–2009 seasonal inactivated influenza vaccines as described (Moody et al., 2011). Those characterized as bnAb producers had broad neutralizing plasma antibodies by previously described criteria from the CHAVI chronic HIV-1 infection cohort (Tomaras et al., 2011) and/or had bnAbs isolated from blood B cells as described (Shen et al., 2009; Morris et al., 2011). PBMC samples were used for DNA isolation for HTS from the influenza vaccinated individuals taken before and 7 days and 21 days after vaccination (Moody et al., 2011) using the methods as described previously (Wrammert et al., 2008; Liao et al., 2009; Moody et al., 2011). All work related to human subjects was in compliance with Institutional Review Board protocols approved by the Duke University Health System Institutional Review Board.

Inference of Unmutated Common Ancestor and Identification of Clone Members

The inference of the $V_H DJ_H$ and $V_L J_L$ of the unmutated common ancestor (UCA) and intermediate antibodies of CD4BS bnAb VRC-CH30-34 clonal lineage is described in detail elsewhere (Kepler, 2013; Kepler et al., 2014). Briefly, we parameterize the VDJ rearrangement process in terms of its gene segments, recombination points, and n-regions. Given any multiple sequence alignment A for the set of clonally related genes and any tree T describing a purported history, we compute the likelihood for all parameter values, and subsequently the posterior probabilities on the rearrangement parameters conditional on A and T. We can then find the UA with the greatest posterior probability and compute the maximum likelihood alignment $A*$ and tree $T*$ given this UA, and then recompute the posterior probabilities on rearrangement parameters conditional on $A*$ and $T*$. We iterate the alternating conditional optimizations until convergence is reached.

To infer likely clonal relatedness, we use the following statistical procedure. Two sequences are regarded as potential relatives if they are inferred to have used the same IGHV and IGHJ genes (without regard to allelic differences) and if the number of differences between the two sequences in their CDR3 is not so large that the following hypothesis is rejected. The hypothesis is that the two CDR3 evolved from a common precursor and that along each of the two branches, the mutation frequency is as estimated from the count of point mutations in IGHV alone. The test itself is a z test based on the Gaussian approximation to the binomial.

Isolation of $V_H DJ_H$ and V_L Genes and Expression of $V_H DJ_H$ and $V_L J_L$ Genes as Full-Length IgG1 Recombinant Monoclonal Antibodies

The $V_H DJ_H$ and $V_L J_L$ gene segment pairs were isolated by RT/PCR from sorted single plasma cells from PBMC collected from healthy blood donors and from vaccinees 7 days after vaccination with either the 2007–2008 or 2008–2009 inactivated influenza vaccine according to a protocol approved by the Duke University Health System Institutional Review Board (Moody et al., 2011). The $V_H DJ_H$ and $V_L J_L$ gene segment pairs of the observed VRC-CH30-34 were obtained as described previously (Wu et al., 2011). Additional $V_H DJ_H$ were identified by HTS (Wu et al., 2011; Boyd et al., 2009). Clonally related sequences derived from the observed CH31-34 and from the cDNA HTS were combined and used to generate maximum-likelihood phylogenetic trees (Figure 3C). The $V_H DJ_H$ gene sequences identified by HTS indicated in blue boxes in Figure 1C have been synthesized and paired with intermediate-4 light chain for production of recombinant monoclonal antibodies (mAbs) for testing the binding and neutralizing activity using the method as described previously (Liao et al., 2011, 2013).

Structural Analysis

A set of 11 antigen-bound structures for the following indel-containing bnAbs were included in the analysis: VRC01, VRC03, VRC-CH31, VRC-PG04, NIH45-46, 3BNC117, VRC-PG20, CH103, PG9, PGT128, and PGT135 (Wu et al., 2010; Bonsignori et al., 2012; Falkowska et al., 2012; Scheid et al., 2011; Chuang et al., 2013; Walker et al., 2009, 2011; Liao et al., 2013). A total of 18 indels were found in the 11 antibodies. For a given antibody, the distance between an insertion and the corresponding antigen was computed as the minimum heavy-atom (C, N, O, and S) distance between any residue part of the insertion and any residue/glycan part of the antigen. Similarly, the distance between an antibody deletion and the corresponding antigen was computed as the minimum heavy-atom distance between either residue flanking the deletion and any residue/glycan part of the antigen. For a given antibody, loop residues were defined by the loop, bend, and turn categories in DSSP (Kabsch and Sander, 1983), with distances computed as the minimum heavy-atom distance between each loop residue and any residue/glycan in the corresponding antigen. In the above analysis, missing residues in the input structure were ignored.

Surface Plasmon Resonance Affinity and Kinetics Measurements

Binding K_d and rate constant (association rate k_a, dissociation rate k_d) measurements of recombinant mAbs of VRC-CH30-34 clonal lineage to A244 Δ11 gp120 (Liao et al., 2013; Alam et al., 2013) were carried out on BIAcore

3000 instruments as described previously (Alam et al., 2007, 2008, 2011). All data analysis was performed using the BIAevaluation 4.1 analysis software (GE Healthcare).

Neutralization Assays

Neutralizing antibody assays in TZM-bl cells were performed as described previously (Montefiori, 2005). Neutralizing activity of plasma samples in eight serial 3-fold dilutions starting at 1:20 dilution and for recombinant mAbs in eight serial 3-fold dilutions starting at 50 ug/ml were tested against autologous and heterologous HIV-1 Env-pseudotyped viruses in TZM-bl-based neutralization assays using the methods as described (Montefiori, 2005; Seaman et al., 2010). The data were calculated as a reduction in luminescence units compared with control wells and reported as IC_{50} in μg/ml for mAbs.

SUPPLEMENTAL INFORMATION

Supplemental Information includes Supplemental Experimental Procedures and three tables and can be found with this article online at http://dx.doi.org/10.1016/j.chom.2014.08.006.

AUTHOR CONTRIBUTIONS

T.B.K. designed the indel studies, performed antibody gene sequence analyses and other statistical analyses, and wrote and edited the paper. H.X.L. produced recombinant antibodies and HIV-1 Envs, designed assays, analyzed data, and wrote and edited the paper; S.M.L. performed SPR analysis; R.B. and C.Y. assisted with antibody gene sequence analysis; R.R.Z. isolated and produced antibodies; S.S. and K.A. performed SPR assays; R.P., K.E.L., and C.S. performed immunoassays; J.P., E.S., and E.F performed antibody and HIV-1 Env production; L.M., S.S.A.K., and M.S.C. provided PBMC samples of HIV-1-infected bnAb individuals; G.K. contributed to the design of the experiments; E.W. carried out influenza vaccination and sample collection from influenza vaccinees; M.A.M. performed single plasma cell sorting for isolation of $V_H DJ_H$ and $V_L J_L$ genes from healthy blood donors and influenza vaccinees; X.W. isolated VRC-CH30-34 bnAbs, H.R.A.-T., I.S.G., and P.D.K., perform the structure analysis, S.D.B. and A.Z.F. performed HTS; J.R.M. isolated antibodies, designed assays, analyzed data, and edited the paper; B.F.H. designed and directed the immunologic and clinical studies, directed the overall study, analyzed data, and wrote and edited the paper.

REFERENCES

Alam, S.M., McAdams, M., Boren, D., Rak, M., Scearce, R.M., Gao, F., Camacho, Z.T., Gewirth, D., Kelsoe, G., Chen, P., and Haynes, B.F. (2007). The role of antibody polyspecificity and lipid reactivity in binding of broadly neutralizing anti-HIV-1 envelope human monoclonal antibodies 2F5 and 4E10 to glycoprotein 41 membrane proximal envelope epitopes. J. Immunol. 178, 4424–4435.

Alam, S.M., Scearce, R.M., Parks, R.J., Plonk, K., Plonk, S.G., Sutherland, L.L., Gorny, M.K., Zolla-Pazner, S., Vanleeuwen, S., Moody, M.A., et al. (2008). Human immunodeficiency virus type 1 gp41 antibodies that mask membrane proximal region epitopes: antibody binding kinetics, induction, and potential for regulation in acute infection. J. Virol. 82, 115–125.

Alam, S.M., Liao, H.X., Dennison, S.M., Jaeger, F., Parks, R., Anasti, K., Foulger, A., Donathan, M., Lucas, J., Verkoczy, L., et al. (2011). Differential reactivity of germ line allelic variants of a broadly neutralizing HIV-1 antibody to a gp41 fusion intermediate conformation. J. Virol. 85, 11725–11731.

Alam, S.M., Liao, H.X., Tomaras, G.D., Bonsignori, M., Tsao, C.Y., Hwang, K.K., Chen, H., Lloyd, K.E., Bowman, C., Sutherland, L., et al. (2013). Antigenicity and immunogenicity of RV144 vaccine AIDSVAX clade E envelope immunogen is enhanced by a gp120 N-terminal deletion. J. Virol. 87, 1554–1568.

Bonsignori, M., Hwang, K.K., Chen, X., Tsao, C.Y., Morris, L., Gray, E., Marshall, D.J., Crump, J.A., Kapiga, S.H., Sam, N.E., et al. (2011). Analysis of a clonal lineage of HIV-1 envelope V2/V3 conformational epitope-specific broadly neutralizing antibodies and their inferred unmutated common ancestors. J. Virol. 85, 9998–10009.

Bonsignori, M., Montefiori, D.C., Wu, X., Chen, X., Hwang, K.K., Tsao, C.Y., Kozink, D.M., Parks, R.J., Tomaras, G.D., Crump, J.A., et al. (2012). Two distinct broadly neutralizing antibody specificities of different clonal lineages in a single HIV-1-infected donor: implications for vaccine design. J. Virol. 86, 4688–4692.

Boyd, S.D., Marshall, E.L., Merker, J.D., Maniar, J.M., Zhang, L.N., Sahaf, B., Jones, C.D., Simen, B.B., Hanczaruk, B., Nguyen, K.D., et al. (2009). Measurement and clinical monitoring of human lymphocyte clonality by massively parallel VDJ pyrosequencing. Sci. Transl. Med. 1, 12ra23.

Briney, B.S., Willis, J.R., and Crowe, J.E., Jr. (2012). Location and length distribution of somatic hypermutation-associated DNA insertions and deletions reveals regions of antibody structural plasticity. Genes Immun. 13, 523–529.

Chuang, G.Y., Acharya, P., Schmidt, S.D., Yang, Y., Louder, M.K., Zhou, T., Kwon, Y.D., Pancera, M., Bailer, R.T., Doria-Rose, N.A., et al. (2013). Residue-level prediction of HIV-1 antibody epitopes based on neutralization of diverse viral strains. J. Virol. 87, 10047–10058.

Eichler, E.E. (1998). Masquerading repeats: paralogous pitfalls of the human genome. Genome Res. 8, 758–762.

Falkowska, E., Ramos, A., Feng, Y., Zhou, T., Moquin, S., Walker, L.M., Wu, X., Seaman, M.S., Wrin, T., Kwong, P.D., et al. (2012). PGV04, an HIV-1 gp120 CD4 binding site antibody, is broad and potent in neutralization but does not induce conformational changes characteristic of CD4. J. Virol. 86, 4394–4403.

Fukita, Y., Jacobs, H., and Rajewsky, K. (1998). Somatic hypermutation in the heavy chain locus correlates with transcription. Immunity 9, 105–114.

Gotoh, O. (1990). Optimal sequence alignment allowing for long gaps. Bull. Math. Biol. 52, 359–373.

Haynes, B.F., Fleming, J., St Clair, E.W., Katinger, H., Stiegler, G., Kunert, R., Robinson, J., Scearce, R.M., Plonk, K., Staats, H.F., et al. (2005). Cardiolipin polyspecific autoreactivity in two broadly neutralizing HIV-1 antibodies. Science 308, 1906–1908.

Haynes, B.F., Moody, M.A., Liao, H.X., Verkoczy, L., and Tomaras, G.D. (2011). B cell responses to HIV-1 infection and vaccination: pathways to preventing infection. Trends Mol. Med. 17, 108–116.

Haynes, B.F., Kelsoe, G., Harrison, S.C., and Kepler, T.B. (2012). B-cell-lineage immunogen design in vaccine development with HIV-1 as a case study. Nat. Biotechnol. 30, 423–433.

Hraber, P., Seaman, M.S., Bailer, R.T., Mascola, J.R., Montefiori, D.C., and Korber, B.T. (2014). Prevalence of broadly neutralizing antibody responses during chronic HIV-1 infection. AIDS 28, 163–169, http://dx.doi.org/10.1097/QAD.0000000000000106.

Kabsch, W., and Sander, C. (1983). Dictionary of protein secondary structure: pattern recognition of hydrogen-bonded and geometrical features. Biopolymers 22, 2577–2637.

Kepler, T.B. (2013). Reconstructing a B-cell clonal lineage. I. Statistical inference of unobserved ancestors. F1000Res *2*, 103.

Kepler, T.B., Munshaw, S., Wiehe, K., Zhang, R., Yu, J.S., Woods, C.W., Denny, T.N., Tomaras, G.D., Alam, S.M., Moody, M.A., et al. (2014). Reconstructing a B-bell clonal lineage. II. mutation, selection, and affinity maturation. Front. Immunol. *5*, 170.

Krause, J.C., Ekiert, D.C., Tumpey, T.M., Smith, P.B., Wilson, I.A., and Crowe, J.E., Jr. (2011). An insertion mutation that distorts antibody binding site architecture enhances function of a human antibody. MBio *2*, e00345–e10.

Kwong, P.D., and Mascola, J.R. (2012). Human antibodies that neutralize HIV-1: identification, structures, and B cell ontogenies. Immunity *37*, 412–425.

Liao, H.X., Levesque, M.C., Nagel, A., Dixon, A., Zhang, R., Walter, E., Parks, R., Whitesides, J., Marshall, D.J., Hwang, K.K., et al. (2009). High-throughput isolation of immunoglobulin genes from single human B cells and expression as monoclonal antibodies. J. Virol. Methods *158*, 171–179.

Liao, H.X., Chen, X., Munshaw, S., Zhang, R., Marshall, D.J., Vandergrift, N., Whitesides, J.F., Lu, X., Yu, J.S., Hwang, K.K., et al. (2011). Initial antibodies binding to HIV-1 gp41 in acutely infected subjects are polyreactive and highly mutated. J. Exp. Med. *208*, 2237–2249.

Liao, H.X., Bonsignori, M., Alam, S.M., McLellan, J.S., Tomaras, G.D., Moody, M.A., Kozink, D.M., Hwang, K.K., Chen, X., Tsao, C.Y., et al. (2013). Vaccine induction of antibodies against a structurally heterogeneous site of immune pressure within HIV-1 envelope protein variable regions 1 and 2. Immunity *38*, 176–186.

Mascola, J.R., and Haynes, B.F. (2013). HIV-1 neutralizing antibodies: understanding nature's pathways. Immunol. Rev. *254*, 225–244.

Montefiori, D.C. (2005). Evaluating neutralizing antibodies against HIV, SIV, and SHIV in luciferase reporter gene assays. Curr. Protoc. Immunol. *Chapter 12*, 11.

Moody, M.A., Zhang, R., Walter, E.B., Woods, C.W., Ginsburg, G.S., McClain, M.T., Denny, T.N., Chen, X., Munshaw, S., Marshall, D.J., et al. (2011). H3N2 influenza infection elicits more cross-reactive and less clonally expanded anti-hemagglutinin antibodies than influenza vaccination. PLoS ONE *6*, e25797.

Moore, P.L., Gray, E.S., Sheward, D., Madiga, M., Ranchobe, N., Lai, Z., Honnen, W.J., Nonyane, M., Tumba, N., Hermanus, T., et al.; CAPRISA 002 Study (2011). Potent and broad neutralization of HIV-1 subtype C by plasma antibodies targeting a quaternary epitope including residues in the V2 loop. J. Virol. *85*, 3128–3141.

Morris, L., Chen, X., Alam, M., Tomaras, G., Zhang, R., Marshall, D.J., Chen, B., Parks, R., Foulger, A., Jaeger, F., et al. (2011). Isolation of a human anti-HIV gp41 membrane proximal region neutralizing antibody by antigen-specific single B cell sorting. PLoS ONE *6*, e23532.

Mouquet, H., and Nussenzweig, M.C. (2012). Polyreactive antibodies in adaptive immune responses to viruses. Cell. Mol. Life Sci. *69*, 1435–1445.

Pejchal, R., Doores, K.J., Walker, L.M., Khayat, R., Huang, P.-S., Wang, S.-K., Stanfield, R.L., Julien, J.-P., Ramos, A., Crispin, M., et al. (2011). A potent and broad neutralizing antibody recognizes and penetrates the HIV glycan shield. Science *334*, 1097–1103.

Scheid, J.F., Mouquet, H., Ueberheide, B., Diskin, R., Klein, F., Oliveira, T.Y., Pietzsch, J., Fenyo, D., Abadir, A., Velinzon, K., et al. (2011). Sequence and structural convergence of broad and potent HIV antibodies that mimic CD4 binding. Science *333*, 1633–1637.

Seaman, M.S., Janes, H., Hawkins, N., Grandpre, L.E., Devoy, C., Giri, A., Coffey, R.T., Harris, L., Wood, B., Daniels, M.G., et al. (2010). Tiered categorization of a diverse panel of HIV-1 Env pseudoviruses for assessment of neutralizing antibodies. J. Virol. *84*, 1439–1452.

Shen, X., Parks, R.J., Montefiori, D.C., Kirchherr, J.L., Keele, B.F., Decker, J.M., Blattner, W.A., Gao, F., Weinhold, K.J., Hicks, C.B., et al. (2009). In vivo gp41 antibodies targeting the 2F5 monoclonal antibody epitope mediate human immunodeficiency virus type 1 neutralization breadth. J. Virol. *83*, 3617–3625.

Smith, D.S., Creadon, G., Jena, P.K., Portanova, J.P., Kotzin, B.L., and Wysocki, L.J. (1996). Di- and trinucleotide target preferences of somatic mutagenesis in normal and autoreactive B cells. J. Immunol. *156*, 2642–2652.

Tomaras, G.D., Binley, J.M., Gray, E.S., Crooks, E.T., Osawa, K., Moore, P.L., Tumba, N., Tong, T., Shen, X., Yates, N.L., et al. (2011). Polyclonal B cell responses to conserved neutralization epitopes in a subset of HIV-1-infected individuals. J. Virol. *85*, 11502–11519.

Verkoczy, L., Kelsoe, G., Moody, M.A., and Haynes, B.F. (2011). Role of immune mechanisms in induction of HIV-1 broadly neutralizing antibodies. Curr. Opin. Immunol. *23*, 383–390.

Walker, L.M., Phogat, S.K., Chan-Hui, P.-Y., Wagner, D., Phung, P., Goss, J.L., Wrin, T., Simek, M.D., Fling, S., Mitcham, J.L., et al.; Protocol G Principal Investigators (2009). Broad and potent neutralizing antibodies from an African donor reveal a new HIV-1 vaccine target. Science *326*, 285–289.

Walker, L.M., Huber, M., Doores, K.J., Falkowska, E., Pejchal, R., Julien, J.-P., Wang, S.-K., Ramos, A., Chan-Hui, P.Y., Moyle, M., et al.; Protocol G Principal Investigators (2011). Broad neutralization coverage of HIV by multiple highly potent antibodies. Nature *477*, 466–470.

Wang, C., Liu, Y., Xu, L.T., Jackson, K.J.L., Roskin, K.M., Pham, T.D., Laserson, J., Marshall, E.L., Seo, K., Lee, J.-Y., et al. (2014). Effects of aging, cytomegalovirus infection, and EBV infection on human B cell repertoires. J. Immunol. *192*, 603–611.

Wilson, P.C., de Bouteiller, O., Liu, Y.-J., Potter, K., Banchereau, J., Capra, J.D., and Pascual, V. (1998). Somatic hypermutation introduces insertions and deletions into immunoglobulin V genes. J. Exp. Med. *187*, 59–70.

Wrammert, J., Smith, K., Miller, J., Langley, W.A., Kokko, K., Larsen, C., Zheng, N.Y., Mays, I., Garman, L., Helms, C., et al. (2008). Rapid cloning of high-affinity human monoclonal antibodies against influenza virus. Nature *453*, 667–671.

Wu, X., Yang, Z.Y., Li, Y., Hogerkorp, C.M., Schief, W.R., Seaman, M.S., Zhou, T., Schmidt, S.D., Wu, L., Xu, L., et al. (2010). Rational design of envelope identifies broadly neutralizing human monoclonal antibodies to HIV-1. Science *329*, 856–861.

Wu, X., Zhou, T., Zhu, J., Zhang, B., Georgiev, I., Wang, C., Chen, X., Longo, N.S., Louder, M., McKee, K., et al.; NISC Comparative Sequencing Program (2011). Focused evolution of HIV-1 neutralizing antibodies revealed by structures and deep sequencing. Science *333*, 1593–1602.

Zhou, T., Georgiev, I., Wu, X., Yang, Z.-Y., Dai, K., Finzi, A., Kwon, Y.D., Scheid, J.F., Shi, W., Xu, L., et al. (2010). Structural basis for broad and potent neutralization of HIV-1 by antibody VRC01. Science *329*, 811–817.

Zhou, T., Zhu, J., Wu, X., Moquin, S., Zhang, B., Acharya, P., Georgiev, I.S., Altae-Tran, H.R., Chuang, G.Y., Joyce, M.G., et al.; NISC Comparative Sequencing Program (2013). Multidonor analysis reveals structural elements, genetic determinants, and maturation pathway for HIV-1 neutralization by VRC01-class antibodies. Immunity *39*, 245–258.